International Journal of Multidisciplinary Research and Growth Evaluation.

Estimation of electrical formation factor and porosity from VES for the aquifers in parts of Bayelsa state Nigeria

Amakiri ARC [1*], Amonieah J [2], Otugo VN [3]
Department of Physics, Rivers State University Port Harcourt, Nigeria

* Corresponding Author: **Amakiri ARC**

Article Info

ISSN (online): 2582-7138
Volume: 05
Issue: 03
May-June 2024
Received: 01-04-2024
Accepted: 03-05-2024
Page No: 480-487

Abstract
An attempt has been made to estimate the formation factor and porosity of the Quaternary Alluvial aquifers in parts of Bayelsa State, in Southern Nigeria. Formation factor (*F*) is a very prominent parameter in most Geophysical investigations; it is fundamentally an indispensable factor in the evaluation of the petrophysical characteristics of repositories. The electrical formation factor (or formation resistivity factor), F_a, was evaluated from modelled resistivity data. In this study, the formation factor was estimated following Archie's original formulation and the corrected formation factor F_c, was estimated following the Waxman-Smits model. Formation factor obtained ranges from 1.41-47.5 with an average of 12.49. The spatial distribution of formation factor in the study area as here presented, shows that formation factor is of highest values in the west central parts and lower in the central parts of the Study area. We attribute the relatively low Formation factor values, in some areas to low pore water resistivity, which ranges from 6 - 179 Ωm, with an average of 69.2 Ωm; as well as high bulk resistivity values ranging from 82 - 1894 Ωm, with an average of 441 Ωm. The estimated porosity in the study area ranges from 12 to 57%, at VES stations of 7, 34 and 21. The spatial distribution of the estimated porosity is shown in Fig. 8. The Porosity values obtained from the inversion of VES modelled parameters (Table 1) show that the porosity (φ) values range from 12% to 57%. The spatial distribution map of the estimated porosity is presented in Fig. 8, the Fig. shows that porosity values vary spatially from low values around the west central and south western parts to relatively high values around the north eastern parts of the study area. The calculated porosity values of an aquifer using average resistivity values are considered average porosity values, this is worthy of note because the resistivity values obtained from VES analysis are themselves average values, constructed from all of the smaller scaled heterogeneities within each layer.

Keywords: Repositories, formation factor, alluvial, porosity

1. Introduction

A very prominent parameter in Geoelectric investigation is the formation factor (*F*); it is fundamentally an indispensable factor in the evaluation of the petro physical characteristics of repositories, engineering construction sites, as well as groundwater aquifers.

Understanding the formation factor is essential in using electrical and electromagnetic methods to monitor leachate accumulations and movements both within and around landfills. Specifically, the formation factor allows leachate resistivity, the degree of saturation, and, possibly, even the hydraulic conductivity of the waste to be estimated from non-invasive surface measurements. The concept of formation factor was first introduced by Sundberg (1932) [18], who examined the ratio of rock resistivity to that of a conductive pore fluid.

The ratio of a rock's resistivity when brine fully saturates it to the brine's resistivity is the formation resistivity factor as originally

designated by Archie (1942) [2]. By this definition, *F*, is independent of the resistivity of the Brine that saturates the rock (Wyllie and Rose, 1950) [14]. This definition of *F*, implicitly has the supposition, that, the solid matrix of the formation is a non-conducting (insulator) material. However, if the solid matrix is a conductive, the independence of *F*, on the resistivity of the fluid that saturates it will no longer exist, in such cases a correction factor may be included to accommodate for the conductive solids present in the rock matrix and if this correction is made, it is theoretically possible to determine, F.

The formation resistivity factor is usually determined by various physical parameters and lithological features, including electrical resistivity, pore water resistivity, temperature, viscosity, and extent of pore water saturation etc (Salem 1994; Salem, 2001) [15, 16].

1.1 The study area

Bayelsa State is one of six states (Edo, Bayelsa, Delta, Rivers, Cross Rivers, and Akwa Ibom) that make up the South-South geopolitical zone of Nigeria.

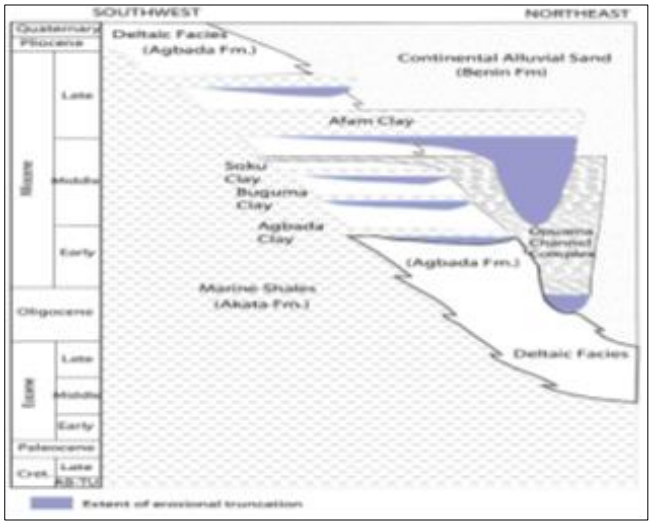

Fig 1: Stratigraphic sequence of the Niger Delta with the three Formations

The name Bayelsa comes from the three previous major local government areas, Yenagoa (Yelga), Brass (Balga), and Sagbama (Salga) (Fig.1). The geographical position of Bayelsa State lies at 4 ° 15 'north latitude and 5 ° 23' south latitude and 5 ° 22 'west longitude and 06 ° 45' east. The state of Bayelsa is a picturesque rainforest having an approximate area of 21,110 Kilometer squared.

Over three quarter of the State is Riverine, characterized by a moderately low-lying land, stretching from Nembe to Ekeremor. The area is almost below sea level, with a labyrinth of winding streams and mangroves. Major rivers in the state are, Ramos, Nun, St. Nicholas, Sangana, Fishtown, Ikebiri Creek; others are, St. Barthelemy, Brass, Pennington, Dobo Middleton and Digatoro Creek; all of which flow into the Atlantic Ocean by a network. of various streams and Rivers (BIPA, 2018) [3].

1.2 Stratigraphy of the Niger Delta region of Nigeria

Bayelsa State is part of the Niger Delta sedimentary Basin, which is located between latitudes 3° - 6°N and longitude 5° - 8°E (Fig.1). The Niger Delta basin Stratigraphically is categorized into three formations known as, Benin, Agbada and Akata, Formations, in order of increasing age (Fig.2). From apex to coast the sub-aerial portion stretches more than 300km, covering an area of 75,000 km^2. The Niger Delta is an active sedimentary basin at present and has prograded since Details of the subsurface of the Niger Delta has fully revealed these three lithostratigraphic units, in the order of the youngest to the oldest, beginning from the Benin to the Agbada and then to the Akata, formation (Short & Stauble, 1967, Uko *et al*. 2002) [7, 20].

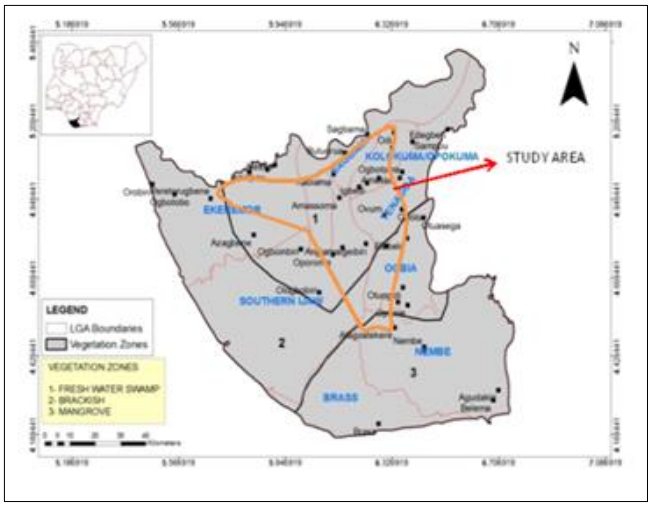

Fig 2: Bayelsa State map with the study area shown (Inset: Bayelsa in map of Nigeria

2. Background Theory

Electrical resistivity techniques have been well-established and ubiquitously employed in resolving various geotechnical, geological, geophysical, environmental and groundwater problems (Amakiri *et al*. 2023 and Ward, 1990) [1, 23]. The primary purpose of the resistivity method is to measure the electric potential on the earth surface as a result of current flow within the earth.

Electric potential distribution in a soil in the vicinity of an electrode carrying current depends on the electric resistivity and the distribution of the surrounding rocks and soils. This basic understanding of physics is the basis for surface electrical resistivity surveying. A schematic of the equipotential surfaces and current lines that results are shown in Figure 2.1. Electric current flow through the ground is a function of several factors, which also depends on the location and the area's geology. The factors comprise of porosity, lithology, grain size, sediment depth, cementation, pore size and geometry, grading, compaction, packing,

groundwater, and groundwater salinity (Salem, 1999, Farid *et al*., 2013) [15, 7].

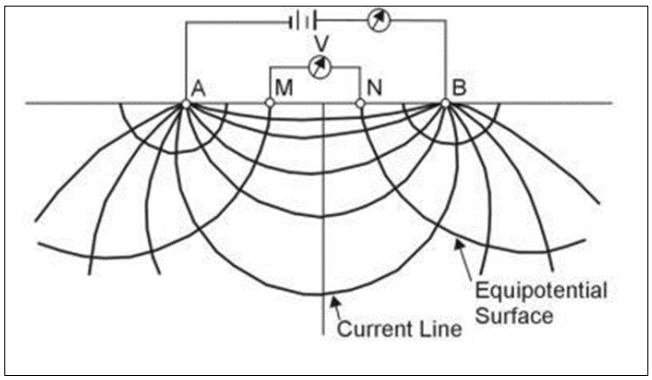

Fig 3: Equipotential and current lines for a pair of current electrodes A and B, and a pair of Potential electrodes M and N, on a homogeneous half-space.

Several configurations for executing the Electrical resistivity survey exists, but the three most employed are shown in Figure 3, which are the Schlumberger, Wenner and the dipole-dipole arrays.

2.1 Vertical Electrical Sounding

The Vertical electrical sounding (VES) is a geoelectric method used for the investigation of the Earth's subsurface, its basic principle helms from the fact that, when current is injected into the Earth by means of two (current) electrodes along a profile line, electric field is generated in the subsurface such that if two other (potential) electrodes are placed appropriately in line with the current electrodes, electric potentials difference can be measured between the two potential electrodes (Fig. 3). Depending on the configuration used, the apparent resistivity of the field investigation can be obtained as a function of the electrode spacing.

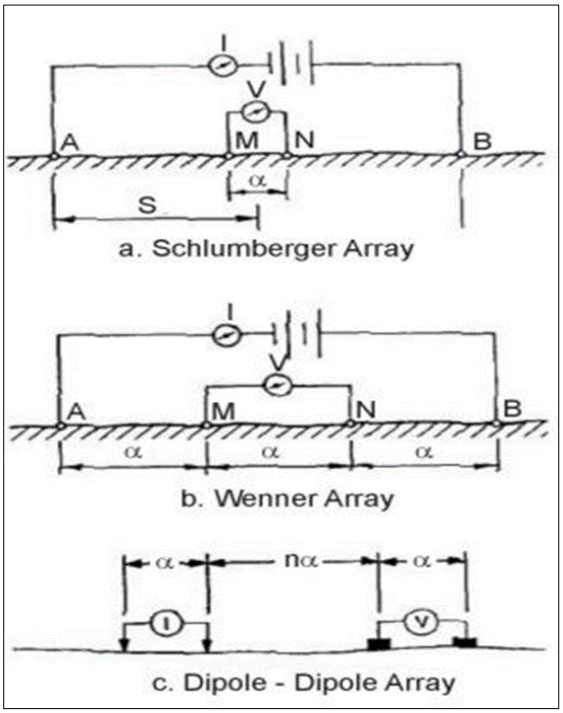

Fig 4: Electrode configurations for resistivity measurements (a) Schlumberger (b) Wenner (c) Dipole-Dipole

2.1.1 The Schlumberger Array

In the Schlumberger array (figure 4), two current electrodes (A and B) are separated a distance apart (AB) and two potential electrodes (M and N) are positioned in between the current electrodes such that the distance from each of the potential electrodes to each current electrode are equal and the center of the array is at the midpoint of M and N.

as α (the potential electrodes interval) tends to zero, the term, V/α, tends to the potential gradient value at the array centre. Practically the instrument's sensitivity has a limitation on the ratio of, *s*, (the distance between the centre of the potential electrodes (the centre electrode) and one of the current electrodes to α, and most often the range will be between 3 and 30. It is usually practicable, therefore, to use an electrode spacing that is finite with equation 2.15 to evaluate the geometric factor (Keller and Frischknecht, 1966) [12]. Consequently, the apparent resistivity (ρ_a) can be given as:

$$\rho_a = \pi\left[\frac{s^2}{\alpha} - \frac{\alpha}{4}\right]\frac{V}{I} = \pi\alpha\left[\left(\frac{s}{\alpha}\right)^2 - \frac{1}{4}\right]\frac{V}{I} \quad (1)$$

Where, s is the distance between the midpoint of M and N and either of the current electrodes, A or B. The inner (potential) electrodes remain fixed in typical field operations, as the outside (current) electrodes are shifted with the distance, *s*. The spacing, α, can only be altered when the sensitivity of the instrument's measurement decreases. The spacing α should not be greater than 0.4*s* otherwise the assumption of a potential gradient will no longer be tenable. Again the, α – spacing, can be varied, sometimes, without changing *s*, so that the detection of local in homogeneities or lateral variations present in the vicinity of the potential electrodes can be possible. For equal electrode spacing as in the Schlumberger configurations, the geometric factor, G, in Equ. 1 becomes,

$$G = \frac{\pi}{4}\left[\frac{AB^2 - MN^2}{MN}\right] \quad (2)$$

Since in the Shlumberger configuration, the current electrode (AB) is usually much larger than the potential electrode (MN), Equ. (2) can be reduced to,

$$G = \frac{\pi}{MN}\left(\frac{AB}{2}\right)^2 \quad (3)$$

Equation (3) can also be expressed as;

$$G = \pi\frac{a^2}{b}\left[1 - \frac{b^2}{4a^2}\right] \quad (4)$$

Where, a = AB/2 and b= MN

When the formation geology is governed only by the vertical variation of the resistivity, a smooth curve will always result when the apparent resistivity is plotted against the configuration spacing. Inversions of resistance and irregularities in apparent resistivity curves, if not caused by errors, both point to lateral changes which would need to be further studied. When the Schlumberger arrangement is used, changing the potential electrode spacing may produce a displacement in the apparent resistivity curve due to lateral inhomogeneity. Such displacement can occur as a general displacement of the curve with no significant change of shape (Zohdy, 1968) [26].

3. Methodology

The methods used in obtaining the results presented in this study are here enumerated.

3.1 Vertical Electrical Sounding (VES)

The vertical electrical sounding was executed in thirteen stations (VES1 to VES13) in the study, using the Schlumberger configuration.

3.1.1 Vertical Electrical Sounding (VES)

The basic objective in caring out a VES survey is to inverse the acquired field data so as to correspond to a subsurface geological or hydrogeological structure. To achieve this aim, it is important to adequately and satisfactorily interpret the acquired field date. The interpretation of VES field data can be implemented in two distinct ways, qualitatively or quantitatively. In the qualitative interpretation approach, the objective is to obtain the thickness and resistivity of the various geologic layers encountered. This is usually achieved analytically, empirically and semi empirically. While in the qualitative VES interpretation approach, the aim is to acquire information on the geological structure of the area under investigation. In this approach, 2D resistivity imaging and contour maps of different types are used to elucidate the detailed structures of the subsurface.

3.1.2 Instrumentation

The equipment used in this study was a commercially available DC Terrameter SAS 1000 (Abem, Sweden). This equipment is a signal averaging system (SAS) resistivity measuring instrument, with reasonably high sensitivity. The Terrameter is rugged, user friendly and easy to carry about; it has been established that the equipment is very efficient, by reason of numerous uses in several investigation sites in Nigeria. The power source to the Abem Terrameter was a 12V battery and four stainless steel metal rods were used as the electrodes.

3.1.3 Data Acquisition and Analysis

Twenty-one Vertical Electrical Soundings (VES) were executed with the DC resistivity meter (Abem Terrameter SAS 1000, (Fig. 3.2) making use of the Schlumberger configuration (Fig. 2.4). All the VES points were located in the vicinity of newly dug or preexisting boreholes, where geologic information was available. The Maximum current electrode half-spacing (AB/2) used ranged between 30 and 250 m (i.e AB ranged from 60 – 500 m) with the assumption that depth penetration ranges between 0.25 AB and 0.5 AB. The centre point of the electrode array remained constant while the spacing of the electrodes was increased in order to obtain information from the successive greater depths.

The current electrode separation (AB/2) followed the sequence: 1.0, 1.5, 2.0, 2.5, 3.2, 4.0, 5.0, 6.0, 7.0, 8.0, 10.0, 12.0, 15.0, 20.0, 25.0, 30.0, 40.0, 50.0, 60.0, 70.0, 80.0, 100.0, 120.0, 150.0, 200.0, while the potential electrode spacing (MN/2) was in the sequence: 0.3, 0.5, 1.0, 1.5, 2.5, 5.0, 7.5, 10.0, 15.0, and 25.0.

Data obtained using the Schlumberger configuration are mostly acquired in overlying segments since at each increasing level of the AB spacing, the signal output from the resistivity meter becomes weaker and weaker, consequently the potential electrode spacing (MN) needed to be increased too and usually the AB/2 values are measured twice, each for the short and long MN spacing. The Schlumberger configuration was used not only because it is faster and most unlikely to be influenced by lateral variations, but also because it involves a minimum number of operators (because the current electrodes, A and B, are displaced away from themselves leaving the potentials electrodes, M unaffected).

The resistance (R) values obtained directly from the field survey served as the primary data which were used for the computation of the apparent resistivity (ρ_a), by employing Equation 5. Von Nostrand and Cook (1984) has observed that, if MN is not more than two-fifth of AB $\left(\frac{2}{5}AB\right)$ then errors in apparent resistivity values will usually range from 2%-3%. The geometric factor (G) used to obtain the apparent resistivity was obtained using Equation (3). The Apparent resistivity values were plotted against the half current electrode spacing (AB/2) on a log-log scale. Guided by the general trend of the field curves, partial curve smoothening of the field curves were generated using the software IPI2win (2000) - a 1D resistivity interpretation software - and Interpex (1DXD). These plots constitute the field curves. The data obtained were later subjected to a computer assisted iterative interpretation using a 1D inversion technique software (1X1D, Interpex, USA) to obtain the one dimensional resistivity model for the area. This program utilizes the least-squares optimization technique, whereby the initial software model is successively adjusted until the difference between the observation and the output of the model is minimized. This program converts (or models) the field acquired apparent resistivities, as a function of the spacing of the electrode, to real resistivities, as a function of the depth. The field data is iteratively matched to a model curve calculated by the program. To build a model with the software, the interpreter subdivides the basement arbitrarily into several horizontal layers of different thicknesses. The resistivities are then iteratively modified by the program to obtain a better fit with the field data for the layer thicknesses chosen for the model. The resulting real resistivities represent the best average resistivity for the given layer.

Fig 5: Abem Terrameter and accessories (a. typical Abem Terrameter b. Typical accessories c. Abem Terrameter (SAS 1000) used in this study, d. Garmin etrex GP*S* used in the study).

3.2 Formation Resistivity factor

The electrical formation factor (or formation resistivity factor), F_a, was evaluated from the modelled field resistivity data following the expression given by Archie (1942) [2].

$$F_a = \frac{\rho_b}{\rho_w} = a\phi^{-m} \quad (5)$$

Where, *a*, is the pore geometry (or texture factor), usually ranging from 0.5 to 1.5; ρ_w, is the resistivity of the pore water; ρ_b is the aquifer bulk resistivity, φ, is porosity (as a volume fraction) and *m*, in the original definition of Archie (1942) [2], is an exponent usually greater than 1.3. The term cementation factor for the exponent, *m*, was introduced by Guyod (1944) [9] since it may be qualitatively shown that formation factor tends to increase as the sand becomes more cemented, for any given porosity. Formation factor varies from unity (1) when the bulk resistivity equals the aquifer water resistivity, (at which instant the porosity is also unity) and increases as the porosity decreases. The formation factor is approximately constant for a given formation and is rarely less than unity, a situation that can only occur when the bulk resistivity is less than the aquifer water resistivity (Glover, 2015) [8].

To evaluate the formation factor, we used bulk resistivity (ρ_b) values, obtained from the 1-D resistivity inversion while the measured pore water resistivity (ρ_w) values, were obtained from bore holes in the vicinity of VES locations, which were taken to the laboratory, were the aquifer conductivity (σ) was obtained and then converted to resistivity using the relation, Farid, *et al*., (2013) [7]:

$$\rho = \frac{1000}{\sigma} \quad (6)$$

Available literature (e.g Waxman and Smits, 1968; Okiongbo and Soronnadi-Ononiwu, (2015) [22, 13] shows that this Archie's relation is only valid for clean, clay-free sand sediments; hence the necessity for the compensation of the clay presence effect; which was achieved in this paper by introducing a correction factor to the formation factor.

The study of the influence of clay content in geophysical parameters began with the work of Patnode and Wyllie (1950) [14], followed by Winsauer and McCardell (1953) [24], Hill and Milburn (1956) [10], and Waxman and Smits (1968) [22]. These works surmised that, when there are conductive materials between grains, the obtained factor is an *apparent* formation factor, in which case an analogy with electrical circuits can be adopted to calculate the formation factor of Clayey or Shaly formations (Diaz-Curiel *et al.* 2016) [5].

3.2.1 Apparent formation factor, F_a, and corrected formation Factor, F_c

In this study, the corrected formation factor F_c, was estimated following the Waxman-Smits (1968) [22] model, which is given as;

$$\frac{1}{F_a} = \frac{1}{F_c} + \left(\frac{BQ_y}{F_c}\right)\rho_w \quad (7)$$

In Equ.7, the coefficient BQ_v is associated with the influences of surface conduction, basically resulting from the presence of clay particles, and when particles of clay are completely absent, the, F_a becomes equal to the corrected formation factor, F_c, (Supious, 2007; Okiongbo and Soronnadi-Ononiwu, 2015) [19, 13]. The inverse of the formation factor in Equation 3; is called the, conductivity formation factor' of the 'connectedness of the rock, and it is the ratio of the fully saturated rock to that of the fluid/water (Glover, 2015) [8]. If $1/F_a$ is plotted against pore fluid resistivity ρ_w, a straight line graph is obtained in which the intercept of the straight line is represented by $1/F_c$, and the slope of the resulting curve is represented by the value of BQ_v/F_c (Devarajan *et al*., 2006) [6]. Hence if 1/Fa is plotted against the aquifer water resistivity (ρ_w), a value for the corrected formation factor (1/Fc) was obtained (Table 1).

3.3 Porosity estimation from VES data

Porosity of the aquifer was estimated from VES data by use of the modified Archie's Equation, after Soupios (2007),

$$\phi = e^{\frac{1}{m}\ln(a) + \frac{1}{m}\ln\left(\frac{1}{F_c}\right)} \quad (8)$$

Where, ϕ, is the porosity, *m* is the cementation factor and *a* is the pore geometry (coefficient of lithology), and F_c is the corrected formation factor. The values of the pore geometry, *a*, and the cementation factor, *m*, as obtained, from grain size porosities, were 0.65 and 1.98 respectively. The resulting porosities are shown in Table 1.

4.0 Results and Discussion

The results from the study are are presented as follows;

4.1 Formation factor

A plot of $1/F_a$ against pore water resistivity (ρ_w), is shown in Figure 6; where the established two trends of correlation are, Trend 1:

$$\frac{1}{Fa} = 0.0082\rho w - 0.1232 \quad (9)$$

With a correlation coefficient of, $\mathbf{R^2 = 0.70}$.

And Trend 2,

$$\frac{1}{Fa} = 0.0032\rho_w - 0.1018 \quad (10)$$

Having a correlation factor of, $\mathbf{R^2 = 0.93}$.

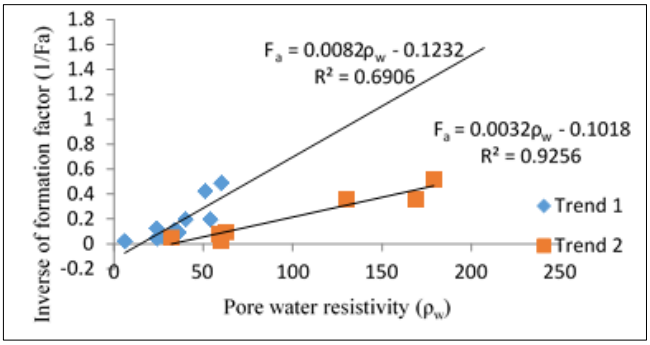

Fig 6: Inverse of formation factor (1/Fa) plotted against pore water resistivity (ρ_w)

The extremely high values of Formation factor in some locations indicates the presence of high bulk resistivity (resistive dispersed phase) and very low Pore water resistivity (conductive continuous phase).

Since the Formation factor (Fa) is dependent on bulk as well as electrolyte resistivity, it is therefore summarily evidenced that Formation factor (F) increases with increase in mean grain size, and consequently higher pore water resistivity (Salem, 2001) [1].

The distribution map of the Formation factor of the study area is shown in Fig. 7. Formation factor evaluated ranges between 1.41 and 47.5 with an average of 12.49 (Table 1). The spatial distribution map of formation factor in the study area is shows that formation factor is of highest values in the east central parts of the study area.

Although Formation factor depends on the behaviour of the porous media, we attribute the relatively low Formation factor values, to low pore water resistivity (which ranges from, 6 - 179 Ωm, average 69.2 Ωm), as well as high bulk resistivity values (ranging from, 82 - 1894 Ωm, average 441 Ωm).

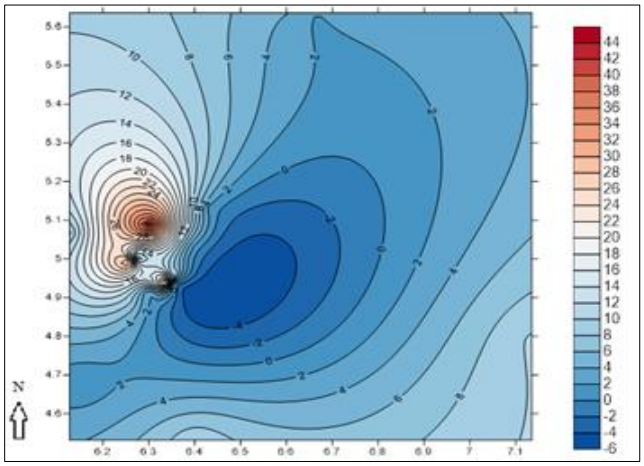

Fig 7: Distribution map of formation factor (Fa) in the study area

4.2 Porosity

The estimated porosity in the study area ranges from 12 to 57%, at VES stations of 7, 34 and 21.

The spatial distribution of the estimated porosity is shown in Fig. 8. The Porosity values obtained from the inversion of VES modelled parameters (Table 1) show that the porosity (φ) values range from 12% to 57%. The spatial distribution map of the estimated porosity is presented in Fig. 8, the Fig. shows that porosity values vary spatially from low values around the west central and south western parts to relatively high values around the north eastern parts of the study area. The calculated porosity values of an aquifer using average resistivity values are considered average porosity values, this is worthy of note because the resistivity values obtained from VES analysis are themselves average values, constructed from all of the smaller scaled heterogeneities within each layer (Soronnadi-Ononiwu, 2015) [13].

Table 1: Estimated formation resistivity factor and intrinsic formation factor (Fi)

VESL	ρ_w	ρ_b	σ_b	σ_w	F_a	$1/F_a$	$1/F_c$	ϕ_{VES}	ϕ_{VES} (%)
2	59	737.5	0.0014	170	12.50	0.08	0.10	0.25	25
3	43	1893.9	0.0005	168	31.3	0.03	0.10	0.25	25
4	51	120.9	0.0083	197	2.37	0.14	0.24	0.39	39
5	135	1000.0	0.0010	74	7.41	0.14	0.28	0.42	42
6	130	364.8	0.0027	77	2.81	0.36	0.04	0.16	16
7	6	285.0	0.0035	1660	47.50	0.02	0.03	0.12	12
8	54	702.4	0.0014	148	21.9	0.05	0.12	0.27	27
9	169	472.9	0.0021	59	2.80	0.36	0.16	0.32	32
10	40	207.0	0.0048	118	20.9	0.18	0.12	0.27	27
11	24	195.5	0.0051	496	20.0	0.05	0.13	0.28	28
12	179	345.9	0.0029	56	1.93	0.52	0.03	0.14	14
13	60	122.8	0.0081	167	2.05	0.02	0.43	0.52	52
14	36	400.0	0.0025	278	11.11	0.03	0.24	0.39	39
16	54	181.0	0.0055	284	1.26	0.19	0.22	0.37	37
17	24	368.0	0.0027	250	1.41	0.04	0.14	0.29	29
18	38	4135.0	0.0002	260	2.11	0.18	0.11	0.25	25
21	180	645.0	0.0016	160	10.32	0.05	0.50	0.57	57
22	34	103.9	0.0096	2300	17.78	0.09	0.17	0.32	32
26	48	298.0	0.0034	295	8.79	0.11	0.25	0.40	40
33	63	645.0	0.0160	160	1.89	0.1	0.40	0.50	50
34	27	290.0	0.0034	583	16.91	0.06	0.02	0.12	12

4.3 Formation factor correlated with Porosity

Formation factor plotted against porosity (φ) is presented in Fig. 9. Fig. 9 shows that Formation factor is related to porosity (φ) in an inverse fashion. The associated regression equation is expressed as;

$F_a = 204 - 5.94\varphi$ (11)

And has a correlation coefficient (R^2) of 0.70.

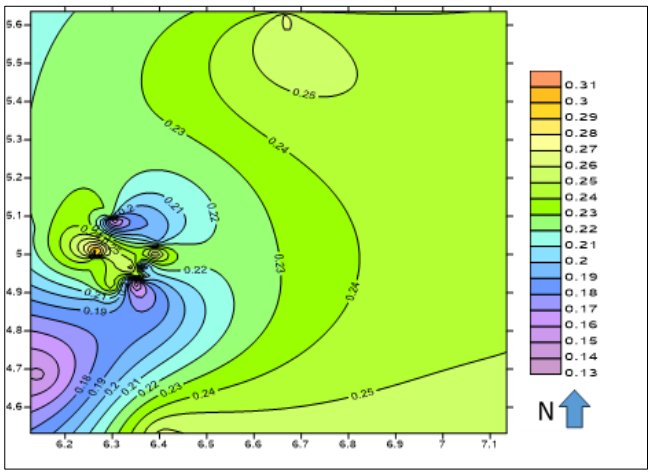

Fig 8: Distribution map of VES porosity (fractional)

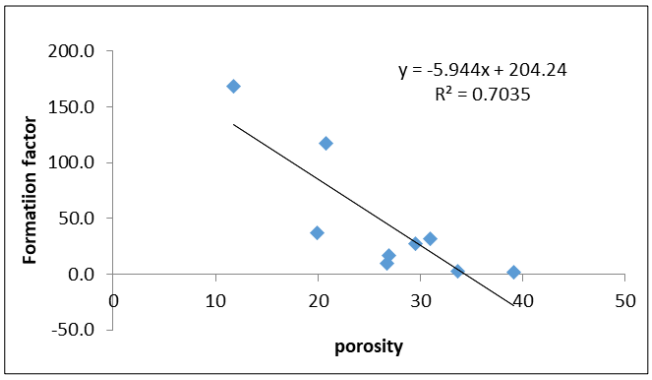

Fig 9: Formation factor against porosity

Conclusion

Electric formation factor and porosity are vital aquifer hydraulic parameters in the geosciences. The present study has undertaken an estimation of formation factor and porosity from Vertical Electrical sounding survey.

Formation factor (Fa) is dependent on bulk resistivity as well as aquifer electrolyte resistivity, it is therefore summarily evidenced that Formation factor (F) increases with increase in mean grain size, and consequently higher pore water resistivity (Salem, 2001) [16]. The spatial distribution map of formation factor in the study area shows that formation factor is of highest values in the east central parts of the study area. The study further reveals that porosity values vary spatially from low values around the west central and south western parts to relatively high values around the north eastern parts of the study area.

Acknowledgment

The authors duly acknowledge the role of the lead author in providing the data used in this study and also to Prof. K. S. Okiongbo, for his intellectual contributions in undertaking the study.

References

1. Amakiri ARC, Risi I, Okiongbo KS. Estimation of grain size statistical parameters and Porosity of the Quaternary aquifers in part of Bayelsa State Nigeria. International Journal of Novel Research in Civil and Structural Engineering and Earth Sciences. 2023;10(2):14-23. Available from: www.noveltyjournals.com
2. Archie GE. The electrical resistivity log as an aid in determining some reservoir characteristics. American Institute of Mining and Metallurgical Engineers Technical Publication. 1942;1422(1):8-13.
3. Bayelsa state investment promotion agency. BIPA; c2018. Available from: www.investbayelsa.by.gov.ng
4. Carpenter JP, Aizhong D, Lirong C. Apparent Formation Factor for Leachate-Saturated Waste and Sediments: Examples from the USA and China. Journal of Earth Sciences. 2009;20(3):606-17. DOI:10.1007/s12583-009-0050-z
5. Díaz-Curiel J, Bárbara Biosca B, María Jesús Miguel MJ. Geophysical estimation of Permeability in Sedimentary Media with Porosities from 0 to 50%. Oil & Gas Science and Technology – Revue d'IFP Energies Nouvelles. 2016;71:27. DOI: 10.2516/ogst/2014053
6. Devarajan S, Toumelin E, Torres-Verdín C, *et al*. Pore-Scale Analysis of the Waxman-Smits Shaly Sand Conductivity Model. SPWLA 47th Annual Logging Symposium; c2006. p. 1-9. Available from: https://www.spwla.org/
7. Farid A, Jadoon K, Akhter G, Iqbal MA. Hydrostratigraphy and hydrogeology of the western part of Maira area, Khyber Pakhtunkhwa, Pakistan: A case study by using electrical resistivity. Environmental Monitoring and Assessment. 2013;185:2407-22. DOI: 10.1007/s10661-012-2720-z
8. Glover PW, Hole MJ, Pous J. A modified Archie's law for two conducting phases. Earth and Planetary Science Letters. 2000;180(3-4):369-383.
9. Guyod H. Fundamental Data for the Interpretation of Electric Logs. Oil Weekly. 1944;115(38):21-27.
10. Hill HJ, Milburn JD. Effect of clay and water salinity on electrochemical behavior of reservoir rocks. Transactions of the AIME. 1956;207(01):65-72.
11. IPI2WIN-1D Computer programme. Programme set for 1-D VES data interpretation. Moscow: Department of Geophysics, Geological Faculty, Moscow University; c2000.
12. Keller GV, Frischknecht FC. Electrical method in geophysical prospecting. Oxford: Pergamon Press; c1966.
13. Okiongbo KS, Soronnadi-Ononiwu GC. Estimation of porosity and hydraulic conductivity of shallow quaternary alluvial aquifer in Yenagoa, southern Nigeria, using geoelectrical measurements. Ife Journal of Science. 2015;17(2):499-502.
14. Patnode WH, Wyllie MRJ. The presence of conductive solids in reservoir rocks as factor in electric log interpretation. Petroleum Transactions, American Institute of Mining, Metallurgical, and Petroleum Engineers. 1950;189:47-52.
15. Salem HS. The electric and hydraulic anisotropic behaviour of the Jeanne d'Arc basin repositories. Journal of Petroleum Science and Engineering. 1994;12(1):49-66.
16. Salem HS. Determination of Porosity, Formation Resistivity Factor, Archie Cementation Factor, and Pore Geometry Factor for a Glacial Aquifer. Energy Sources. 2001;23(6):589-96. DOI: 10.1080/00908310152125238
17. Short KC, Stauble AJ. Outline of Geology of the Niger Delta. AAPG Bulletin. 1967;51(5):761-779.
18. Sundberg K. Effect of Impregnating Waters on Electrical Conductivity of Soils and Rocks. Transactions of the American Institute of Mining and Metallurgical

Engineers. 1932;97:367-91.
19. Supious PM, Kouli M, Vallianatos F, Vafidis A, Stavroulakis G. Estimation of aquifer hydraulic parameters from surficial geophysical methods: A case study of Keritis Basin in Chania (Crete – Greece). Journal of Hydrology. 2007;338:122-131.
20. Uko E, Amakiri A, Alagoa K. Effect of lithology on geothermal gradient in OML-11 in Niger Delta. Global Journal of Pure and Applied Sciences. 2002;8(3):325-337.
21. Vukovic M, Soro A. Determination of hydraulic conductivity of porous media from grain-size composition. In: Kasenow M, editor. Determination of Hydraulic Conductivity from Grain Size Analysis. Littleton, CO: Water Resources Publications; c1992.
22. Waxman MH, Smith LJM. Electrical conductivities in oil bearing sands. Journal of the Society of Petroleum Engineers. 1968;8:107-22.
23. Ward SH. Investigations in Geophysics. Vol. 5. Tulsa: Society of Exploration Geophysicists; c1990.
24. Winsauer WO, McCardell WM. Ionic double-layer conductivity in reservoir rock. Transactions of the American Institute of Mining, Metallurgical, and Petroleum Engineers. 1953;198:129-34.
25. Wyllie MRJ, Rose WD. Some theoretical considerations related to the quantitative evaluation of the physical characteristics of reservoir rock from electrical log data. Journal of Petroleum Technology. 1930;2(4):105-118.
26. Zohdy A, Eaton GP, Mabey DR. Application of surface geophysics to ground-water investigations: Techniques of Water-Resources Investigations of the United States Geological Survey. Chapter D1, book 2; c1974. p. 116.